HHS Public Access

Author manuscript

*Science*. Author manuscript; available in PMC 2024 May 07.

Published in final edited form as:

*Science*. 2023 November 17; 382(6672): eadg3053. doi:10.1126/science.adg3053.

# Design principles of 3D epigenetic memory systems

**Jeremy A. Owen**[1,†], **Dino Osmanović**[2], **Leonid Mirny**[1,*]

[1]Department of Physics, Massachusetts Institute of Technology; Cambridge, USA

[2]Department of Mechanical and Aeronautical Engineering, UCLA; Los Angeles, USA

## Abstract

Cells define and remember their identities, in part, using epigenetic marks—chemical modifications placed along the genome. How can mark patterns remain stable over cell generations despite their constant erosion by replication and other processes? We developed a theoretical model which reveals that 3D genome organization can stabilize an epigenetic memory, as long as (1) there is a large density difference between chromatin compartments, (2) modifying "reader-writer" enzymes spread marks in 3D, and (3) the enzymes are limited in abundance relative to their histone substrates. Analogous to an associative memory that encodes memory in neuronal connectivity, mark patterns are encoded in a 3D network of chromosomal contacts. Our model provides a unified account of diverse experimental observations, and reveals a key role of 3D genome organization in the maintenance of epigenetic memory.

## One-Sentence Summary:

The 3D folding of the genome in the nucleus can help cells remember.

## Introduction

Remembering gene expression states—that is, which genes are "on" or "off"—is a striking capability of living cells. It is well-established that this "epigenetic" memory can be stably encoded in the abundances of freely-diffusing transcription factors (TFs) regulating each other's synthesis (1–3). But in eukaryotes, such as ourselves, in addition to TF-based memory, there is evidence that memory can be held locally to the genes, in the chromatin (4–6). It has been suggested that a seat of this chromatin-based epigenetic memory could be the chemical modifications ("marks") of the DNA-bound histones, which vary across the genome in patterns correlated with gene expression. However, chromatin and its marks

*Corresponding author. leonid@mit.edu.

†Present address: Department of Chemistry, Princeton University; Princeton, USA

Author contributions:
Conceptualization: JAO, DO, LM
Methodology: JAO, DO, LM
Investigation: JAO, DO, LM
Funding acquisition: LM
Project administration: LM
Supervision: LM
Writing – original draft: JAO, DO, LM
Writing – review & editing: JAO, DO, LM

**Competing interests:** Authors declare that they have no competing interests.

are subject to huge disruptions through the cell cycle, and it is not clear what is required to make stable memories out of mark patterns. Here, we identify three qualitative elements that together are sufficient for stable epigenetic memory. Our minimal theoretical model incorporating these elements unites a battery of classic observations ascribed to epigenetic memory of heterochromatin, makes predictions that emerging experimental techniques will test, and suggests a functional role for a hallmark of nuclear organization—its 3D compartmentalization.

Heterochromatin—the transcriptionally-silent, denser nuclear compartment—is rich in particular histone marks, especially the lysine trimethylations H3K9me3 and H3K27me3. These marks are made by so-called “reader-writer” enzymes (7, 8) which can bind marked histones allosterically, stimulating their marking activity on neighboring histones, effectively “spreading” marks between neighbors. Marks can be retained locally when the replication fork passes (9, 10), but they are (by necessity) diluted in the process by newly synthesized, unmarked histones. The combination of these two features is highly suggestive of a stable memory system, in which local mark spreading accurately restores mark patterns after their partial erasure at replication. However, simple mathematical models (11, 12) of this mechanism reveal a basic instability—if mark spreading is strong enough to restore a partially erased pattern, marks also spread ectopically to the rest of the chromosome.

Recent experiments suggest that reader-writer enzymes may be able to spread histone marks “in 3D” (8, 13, 14), that is, between histones that are nearby in space because of how chromatin is folded, not just “in 1D” along the chromatin polymer. Since histone marks also contribute to the spatial compartmentalization of the genome, this raises the tantalizing possibility of a *bidirectional* coupling between the 3D folding of chromatin and the marks on the chromatin polymer (15–18). Could this help stabilize memory? Recent theoretical work (18–21) has explored some consequences of this putative coupling, but broadly, these works have trouble achieving a self-sustaining memory of mark patterns. An understanding of the qualitative conditions required for chromatin-based epigenetic memory is yet to emerge.

## Model

In search of design principles for epigenetic memory, we introduce and study a simple biophysical model in which memory will be held autonomously in mark patterns. Importantly, in many prior models, mark patterns are sustained by external reinforcement, for example by “nucleation sites” or “genomic bookmarks” (11, 12, 22) that recruit modifying enzymes, or by a static 3D contact structure (23). But a pattern determined by external influences is not itself a seat of memory, and so we exclude such elements from our model.

We model chromatin as a long polymer of $10^4$ monomers confined within a sphere (Figure 1A). This could coarsely represent all the chromatin in the nucleus, or just a chromosomal region of 2 Mb (i.e. $10^4$ nucleosomes). Monomers in the polymer can be in one of two states—A or B—with B monomers representing marked, heterochromatic regions and A monomers representing unmarked, euchromatic ones. To represent the “stickiness” of heterochromatin (24–27), B monomers experience a short-range attraction (Figure S14) to

one another of magnitude $a$, which leads B monomers to spatially segregate from the A monomers, forming a denser compartment.

To model the 3D spreading of marks (Figure 1B), we suppose that A monomers turn into B monomers at a rate $Sn_B$, where $n_B$ is the number of neighboring B monomers within a 3D interaction radius $r_c$ (1.5 times the diameter of a monomer), and $S$ is the spreading rate. B monomers turn back into A monomers at a constant rate $L$, uniformly at all sites, representing in aggregate the loss of marked histones due to the activity of demodifying enzymes (e.g. demethylases), histone exchange, and replicative dilution (see below). Our core results will prove insensitive to precisely how the loss of marks is modeled (Figure S2).

To represent the cell cycle (Figure 1C), we run our model in two alternating phases. During "mitosis", we assume marks remain unchanged, while the chromatin polymer is compacted into a condensed state. It then expands to form a compartmentalized interphase state. During "interphase", we assume the chromatin is frozen in place while marks are spread and lost, reaching a steady state. Each round of polymer dynamics followed by mark dynamics we call one "cell generation". Our assumptions stylize experimental observations. In interphase, the gross 3D organization of chromatin is quite stable (28), whereas some marks can turn over completely on a timescale of minutes to hours (29, 30)—a time over which chromatin loci may displace by just ~ 0.2 to 0.4 microns (31). In mitosis, by contrast, repressive marks appear to be stable (32, 33), even as chromatin undergoes dramatic changes. Several factors may account for this, including inhibition of modifying enzymes by mitotic phosphorylation of the H3 tail (34, 35), decreased accessibility of mitotic chromatin, and the short duration of mitosis. Later, we will loosen the assumptions we make about the phases (Figure S3, S4).

An initial pattern of A/B monomer identities is set prior to the first interphase, and is allowed to evolve over one or many cell generations. If, at later times, the pattern resembles the initial pattern, *and would do so for several possible initial patterns*, then the system can be said to exhibit memory.

## Results

Over a single cell generation, we find there is an extremely good memory of mark patterns. The steady state of the mark dynamics reached in the "interphase" closely resembles the initial mark pattern used to fold the polymer (Figure 2A and 2B). The steady-state pattern can recover after huge perturbations, such as a complete randomization of the pattern (every monomer is randomly set to A or B) (Figure 2A), or wholesale erasure of half of the pattern (Figure 2B). The reason for the recovery of the pattern is that spreading marks tend to localize to dense regions—the remaining marks spread in 3D and restore the marks in the spatially dense compartment that was formed by the originally marked regions. It is as if the mark pattern has been "memorized" in the 3D configuration of the polymer.

A surprising analogy to epidemic spreading can help us understand the localization of marks to dense regions quantitatively. The mark dynamics of our model are identical to a Susceptible-Infected-Susceptible (SIS) epidemic model on a network (36). The monomers of our polymer are like individuals whose "social" contact network (Figure 2D) is defined

by the polymer configuration and the marked state is like the infected state. The infection, like marks, spreads at a rate $S$ and infected individuals recover (lose marks) at the rate $L$. A key parameter for epidemic spreading dynamics is the average number of neighbors $d$ of an individual (monomer). Roughly, there is an "epidemic threshold" $1/d$, such that if $S/L$ is below $1/d$, the infection will die out.

Returning to our model with a dense and diffuse compartment, with average numbers of neighbors $d_+$ and $d_-$, respectively, this suggests that when $S/L$ lies in the range:

$$\frac{1}{d_+} \leq \frac{S}{L} \leq \frac{1}{d_-}$$

there should be sharp localization of marks to the dense compartment, with very few marks in the diffuse compartment (see Supplementary Text for a more careful discussion). Intuitively, this condition says that the system must be above the "epidemic threshold" in the dense region, and below it in the diffuse region. Consistently, simulations (Figure 2C) show localization of marks in an even broader range of $S/L$. As the strength of self-attraction $a$ increases, the difference in the densities grows (Figure 2C, inset), further broadening this range. The analogy to epidemic spreading shows quantitatively how the density difference between the compartments is key to sharp localization of marks to the dense compartment, providing robust recovery of the initial mark pattern within one cell generation.

However, over multiple generations (Figure 3), something starkly different happens. Sweeping through the parameter space of our model (Figure 3B), what we find is an unstable, all-or-none behavior. When $S/L$ is greater than a critical value $\lambda_c(a)$ (which depends on $a$), an initially marked region grows uncontrollably until it covers the whole polymer. When $S/L$ is less than the critical value, marks are instead lost globally. In both cases, memory of the initial state is lost within a few generations. When there is strong self-attraction and $S/L$ is fine-tuned to very near the critical value, memory lasts longer, but even then there is a clear tendency to uncontrolled spread or global loss of marks. The same basic instability is apparent in the closely related model of Sandholtz et al. (36–38), who found that fine-tuning of parameters was required to achieve just 5 generations of mark pattern memory. Taken together, 3D spread of marks, even when coupled with 3D genome folding through the self-attraction of marks, is not enough to provide lasting epigenetic memory.

But so far, we have neglected a key biological fact, often omitted in biophysical models of mark dynamics. Marks do not spread themselves—spreading requires the action of a reader-writer enzyme, which in the nucleus is likely to be *limited* relative to its histone substrates. Estimates of the abundances of the histone methyltransferases PRC2 and SETB1 (37–39), for example, suggest that they are hundreds to thousands of times less abundant than nucleosomes, which number in the tens of millions. To account for the limitation of the reader-writer enzymes we introduce a Michaelis-Menten-type scheme (40, 41) where A-B pairs that are within the interaction radius act as the substrate (Figure 3F). We find that adding enzyme limitation to our model remarkably stabilizes the memory of the initial

mark pattern (Figure 3D, E) for hundreds of cell generations, and over a broad range of parameters.

The effect of enzyme limitation is to replace the spreading rate $S$ by an effective spreading rate $S_{eff}$ that depends on the number of A-B pairs $N_{AB}$ (Supplementary Text):

$$S_{\text{eff}} = \begin{cases} S & \text{if } N_{AB} < E_T \\ \frac{SE_T}{N_{AB}} & \text{if } N_{AB} \geq E_T \end{cases},$$

where $E_T$ is the total amount of enzyme. Intuitively, the enzyme sets a maximum global modification rate—the "$V_{\max}$" of the enzyme, which equals $SE_T$. Where before marks would spread uncontrollably across the whole polymer, now the total number of marks is set by the balance of $V_{\max}$ and $L$ to be $N_B = SE_T/L$. Strikingly, this fixing of the number of marks is sufficient to yield a stable memory of the mark *pattern*, e.g. the position of a marked domain (Figure 3D, Figure S1). Stability of the mark pattern is also seen when loss occurs purely by replicational dilution (modeled as random loss of half the marks) once every cell cycle period $T_{\text{div}}$ instead of at a constant loss rate $L$ (Figure S2). Importantly, stable memory is seen across a broad range of parameters, as long as self-attraction is strong enough (Figure 3E), and it works without external reinforcement or fine tuning, as required by other models.

To summarize our findings so far, we have found a memory system that depends on three key ingredients—all characteristic of heterochromatin: (i) strong self-attraction of marked regions, leading to nuclear compartmentalization and densification of marked regions; (ii) 3D spread of marks, and; (iii) limitation of the "reader-writer" enzyme, relative to its substrates. Together, we propose that the presence of these elements amounts to a basic design principle for epigenetic memory systems that exploit 3D genome structure for their function. Importantly, our results suggest that heterochromatin may be dense *not* to sterically exclude transcriptional machinery (heterochromatin is likely highly permeable to polymerase-size particles (42)), but rather as a way to maintain the memory of heterochromatin.

A rich observable phenomenology follows directly from these elements, providing strong support for our model, and many new predictions to be tested by emerging experimental modalities.

First and most basically, our model relates the abundance of a mark to the activity ($S$) and concentration ($E_T$) of a reader-writer enzyme that makes it—in particular, we find a broad regime in which the number of marks is *linear* in both these quantities: $N_B = SE_T/L$. This crisp prediction is at least consistent with the measured effects of EZH2 inhibition (43) and activating mutations (44, 45) on H3K27me3 levels (Supplementary Text), although a definitive test of linearity will require very careful quantitation of both sides of the equation. Perhaps more surprisingly, our model reveals that sometimes changing the concentration of an enzyme is different than uniformly changing its activity. This could shed light on mechanistic puzzles, such as the question of how the oncogenic mutant H3K27M histone

reduces H3K27me3—does it sequester limited PRC2 (effectively reducing $E_T$) (46), or does it persistently reduce its activity (e.g. $S$) after transient contact (37)? Our model predicts that varying $E_T$ should change the number of marks smoothly, whereas reducing $S/L$ below a critical value can cause a sharp, global loss of marks (Figure S5).

Second, our model predicts that only about half of monomers in marked regions are marked. As $S/L$ or $E_T$ is varied, the stable mark domains (Figure 3E) arising in the limited enzyme regime vary in length, but the fraction of monomers within the domain that are marked remains roughly constant, around 0.55 (Figure S6A). This "semimarking" phenomenon is consistent with several experimental results. Semimarking leads to a density difference of 2 to 3 fold between compartments (Figure S6B), consistent with observed differences between heterochromatic and euchromatic regions in the nucleus (47). Semimarked domains also fold into irregular structures (Figure S6B) as recently observed in microscopy of Polycomb-repressed *Hox* genes (48), instead of spheres as would fully marked domains. Additionally, semimarking explains the counterintuitive findings of Alabert et al. (49) that certain histone marks require several cell generations to be fully established on new histones after replicational dilution, and that old histones keep getting marked—our model naturally reproduces these observations (Figure S7).

Third, our model predicts a coupling between distant genomic regions, mediated by the titration of the limited enzyme. The plainest consequence of this is that if marks are lost somewhere, they tend to be gained elsewhere. In capturing this, our model agrees with the numerous observations of such titration effects in epigenetic systems (50–52). As one illustration of this, we show that our model (Figure S8) can emulate the findings of Kraft et al. (53) that genomic deletion of PRC2 nucleation sites can cause loss of H3K27me3 local to the deletion but gain of the mark elsewhere.

A more surprising prediction is that this "mark redistribution" has a natural directionality to it—marks tend to flow from smaller domains to larger domains. A pattern consisting of multiple, noncontiguous mark domains can be remembered for hundreds of generations (Figure 4A). However, we observe that over a longer timescale, the separate domains compete with one another for the limited enzyme (even when "infinitely" far apart, Figure S9), inexorably leading to the formation of a single big domain.

The spontaneous formation of a big marked domain by mark redistribution after many cell generations is reminiscent of the formation of senescence-associated heterochromatin foci (SAHF) in senescent cells, which is associated with *loss* of heterochromatin elsewhere (53). Present accounts of SAHF formation suggest an orchestrated process regulated by many specific effectors (54), but our findings highlight the possibility that similar behavior could be a primitive tendency of mark spreading coupled to 3D genome organization.

Longer domains are more stable against mark redistribution in direct proportion to their length (Figure S9). This effect extends to clusters of domains—as the inter-domain separation is decreased, they begin to act as a single larger domain, lasting longer in competition with a larger domain (Figure 4B). These predictions could be tested by

observing the fate of artificial ectopic mark domains of differing lengths (19, 55, 56), and clusters of small marked domains.

Importantly, since tiny domains are lost very quickly, mark redistribution can be viewed as a form of error correction. If “errors” appear in the form of a background rate at which monomers spontaneously switch from A to B—creating “domains” consisting of individual monomers—these errors are corrected immediately by redistribution of the marks to a larger domain (Figure 4C, Figure S10). Resistance to this kind of error is important for any model of epigenetic memory based on spreading by reader-writer enzymes, because these enzymes have (at some low, but nonzero rate) nonspecific “writing” activity, unstimulated by the “reader” domain (57, 58). Conversely, this finding suggests that mechanisms other than ours must be at work in the tiniest, stable mark domains, such as the three nucleosome *FLC* nucleation region of *Arabidopsis* (57, 58). Our model is completely compatible with such mechanisms—introducing small, permanently marked regions to our model does not alter the basic story (Figure S11).

The final category of tests for our model stem from its ability to capture the emergence of epigenetic heterogeneity in a cell population. We consider the case in which marks are initially present in a small contiguous region and then $S/L$ or $E_T$ is suddenly increased (Figure 4D–I). This could represent a developmental event, such as an increase in the duration of the cell cycle (which effectively decreases $L$), or the overexpression/activation of a reader-writer enzyme (an increase in $E_T$). Immediately, new marks emerge randomly along the polymer, but over a few cell generations they redistribute to form one or a few large domains, strongly biased to include the small initially marked domain (Figure 4D). At the level of a population average (Figure 4E) the initial domain appears to simply expand *linearly* into a larger one. But in fact there is large single-cell variation involving noncontiguous domains (Figure 4F), a prediction single-cell epigenomic techniques (59) could test.

Remarkably, this behavior means that our model—without any modification or additional elements—can reproduce both classic and emerging aspects of the position-effect variegation (PEV). In PEV, translocations of the *white* gene of *Drosophila* to a genomic position near or within heterochromatin leads to stochastic, but mitotically-heritable, silencing of the gene (50). This results in a “variegating” phenotype characterized by mottled red-white eyes, where clonal patches bear the same coloration. Thus, the state of the locus is stochastic yet memorized over many cell divisions. To see PEV in our model, we create cell lineage trees by simply duplicating our simulation after every generation, and then continuing the simulation of the copies independently. We then interrogate the marking status of a small “regulatory region” somewhere along the polymer, to read out the silencing status over time in the lineage (Figure 4G–I). Solely by varying the position of this region, relative to the initially marked domain, our model reproduces starkly different observed phenotypes—including both the “sectored” (Figure 4H) and “salt-and-pepper” (Figure 4I) modes of variegation (60, 61)—thus providing a mechanistic rationale for this classic phenomenon of stochastically established yet memorized epigenetic states.

## Discussion

To summarize, the epigenetic memory mechanism we found requires three ingredients: self-attraction of marked regions, 3D spread of marks, and limited enzyme. Our simple model, a *minimal* one containing these ingredients, exhibits rich behavior that qualitatively matches classic experiments and generates predictions for new ones.

Our model makes a number of assumptions and has several limitations, including its consideration of just a single epigenetic mark rather than competing or successive levels of modification, as well as the absence of heterochromatic attraction to the nuclear lamina. Mark patterns can certainly be strongly influenced by processes we do not model here, such as nucleation regions to which modifying enzymes are recruited (61–64), or actively transcribed regions that are impervious to repressive marks (62–65). Our memory mechanism is compatible with such exogenous influences. Simulations in which we impose that some regions are “pinned” to be permanently marked (Figure S11) or conversely, are unmarkable (Figure S12), exhibit stable memory of mark domains away from pinned regions. It is also possible that some genomic elements are required to “license” certain regions for memory (66, 67). Such “conditional nucleation sites” (67) could be modeled as markable regions separated by large unmarkable ones. In fact, in our model, this kind of architecture may help memory by slowing mark redistribution (Figure S11C).

We also explored variants of our model that relax two of our central assumptions: the absence of mitotic mark dynamics and the absence of interphase chromatin dynamics. We find that spreading of marks during mitosis has only a small effect, most fundamentally because mitosis is short in duration relative to the length of the cell cycle (Figure S3, Supplementary Text). This effect compounds (Figure S3B) with any reduced activity of modifying enzymes on mitotic chromatin (e.g. due to reduced chemical or physical accessibility), further diminishing the role of possible mitotic spread of marks. Interphase dynamics can accelerate the loss of mark patterns (especially when loss is solely due to replicative dilution), but we find this can be rescued by increasing the strength of self-attraction (Figure S4, Supplementary Text). Tethering of heterochromatin to the lamina might also play this role, hinting at a mechanism that could link disruptions of the lamina to epigenetic memory (68, 69).

A natural question about epigenetic memory systems is how much information can be stored, and for how long? As a very first step towards addressing this question for our system, we chose a scheme for recording and reading out “bits” in a mark pattern, and then investigated how the probability of a bit error grows over successive cell generations in our model (Figure S13, Supplementary Text). We uncover a capacity-stability tradeoff—the more bits one seeks to encode (in our polymer of fixed length), the shorter the memory. For example, our system can reliably memorize at least 8 bits for 50 generations, or at least 17 bits for 20 generations. Importantly, these are only lower bounds on the capacity, as we have not shown that our scheme for encoding bits is optimal. Errors arise by mark redistribution, and we only poorly understand what controls the redistribution timescale, aside from the expectation that it will increase with system size. Despite these caveats, our estimate gives

us a sense of scale—a mechanism like ours (using only $10^4$ monomers), could provide stability to 250 (~$2^8$) alternative cellular states over 50 generations.

Intuitively, the memory mechanism we uncover relies on the encoding of memory in different forms in different phases of the cell cycle. In interphase, memory is held in the 3D structure of the genome, in the form of density differences, because dynamic marks sharply localize to dense regions. During mitosis, when the 3D structure is being totally reorganized, memory is held in the 1D sequence of marks.

The mark dynamics on a fixed polymer in our model clearly has some affinity to the protein sequence design problem (70–72) where the goal is to find an amino acid sequence that will fold into a target 3D structure. Classically, the design may be accomplished by choosing a sequence that minimizes the energy of the target configuration relative to all other configurations (73, 74). Analogously, our mark dynamics—although not directly minimizing the energy of a target structure—nevertheless performs a kind of sequence design, giving rise to a mark sequence that refolds into a similar polymer structure. The dynamics of our model could then be thought of as iterated rounds of design and refolding, with the goal of preserving the sequence—a problem that is different from sequence design, and that to our knowledge has not been considered in the protein folding field.

The encoding of a mark pattern via folding of the polymer, within one cell generation, could also be thought of as the “learning rule” of an associative memory in a Hopfield network (75). Learning by the Hebb rule in such networks strengthens connections between active neurons (76, 77)—here, connections between marked regions are established by folding them together (“*mark* together, *park* together”). In this analogy, the mark dynamics are like the “update rule” that allows recovery of a stored memory. This lens is particularly relevant with the growing recognition that single cells (78–80) and simple chemical systems (81, 82) are capable of remarkably complex behaviors and memory. The possibility that epigenetic systems are capable not just of memory but also of more sophisticated information processing, such as associative learning, should be kept in mind—it may be the key to understanding them in their full complexity.

## Supplementary Material

Refer to Web version on PubMed Central for supplementary material.

## Acknowledgments:

The authors are very grateful to Mehran Kardar for valuable scientific discussions.

**Funding:**

National Human Genome Research Institute, NIH 3UM1HG011536 (LM)

National Institute of General Medical Sciences, NIH GM114190 (LM)

National Science Foundation 2044895 (LM)

## Data and materials availability:

To simulate our model, we used polychrom (83), a lab-developed wrapper of OpenMM (84) for the polymer dynamics, and EoN (Epidemics on Networks) (85) for the mark dynamics.

## References and Notes


1. Ptashne M, A genetic switch: Gene control and phage. lambda (1986).
2. GIardner TS, Cantor CR, Collins JJ, Construction of a genetic toggle switch in Escherichia coli. Nature. 403, 339–342 (2000). [PubMed: 10659857]
3. Zhu R, del Rio-Salgado JM, Garcia-Ojalvo J, Elowitz MB, Synthetic multistability in mammalian cells. Science. 375, eabg9765 (2021).
4. Berry S, Hartley M, Olsson TSG, Dean C, Howard M, Local chromatin environment of a Polycomb target gene instructs its own epigenetic inheritance. Elife. 4, e07205 (2015). [PubMed: 25955967]
5. Dodd IB, Sneppen K, “Modeling Bistable Chromatin States” in Epigenetics and Systems Biology (Elsevier, 2017), pp. 145–168.
6. Bonasio R, Tu S, Reinberg D, Molecular signals of epigenetic states. Science. 330, 612–616 (2010). [PubMed: 21030644]
7. Margueron R, Justin N, Ohno K, Sharpe ML, Son J, Drury Iii WJ, Voigt P, Martin SR, Taylor WR, De Marco V, Others, Role of the polycomb protein EED in the propagation of repressive histone marks. Nature. 461, 762–767 (2009). [PubMed: 19767730]
8. Müller MM, Fierz B, Bittova L, Liszczak G, Muir TW, A two-state activation mechanism controls the histone methyltransferase Suv39h1. Nat. Chem. Biol 12, 188–193 (2016). [PubMed: 26807716]
9. Reverón-Gómez N, González-Aguilera C, Stewart-Morgan KR, Petryk N, Flury V, Graziano S, Johansen JV, Jakobsen JS, Alabert C, Groth A, Accurate recycling of parental histones reproduces the histone modification landscape during DNA replication. Mol. Cell 72, 239–249 (2018). [PubMed: 30146316]
10. Escobar TM, Oksuz O, Saldaña-Meyer R, Descostes N, Bonasio R, Reinberg D, Active and repressed chromatin domains exhibit distinct nucleosome segregation during DNA replication. Cell. 179, 953–963 (2019). [PubMed: 31675501]
11. Hathaway NA, Bell O, Hodges C, Miller EL, Neel DS, Crabtree GR, Dynamics and memory of heterochromatin in living cells. Cell. 149, 1447–1460 (2012). [PubMed: 22704655]
12. Hodges C, Crabtree GR, Dynamics of inherently bounded histone modification domains. Proceedings of the National Academy of Sciences. 109, 13296–13301 (2012).
13. Oksuz O, Narendra V, Lee C-H, Descostes N, LeRoy G, Raviram R, Blumenberg L, Karch K, Rocha PP, Garcia BA, Others, Capturing the onset of PRC2-mediated repressive domain formation. Mol. Cell 70, 1149–1162 (2018). [PubMed: 29932905]
14. Kraft K, Yost KE, Murphy S, Magg A, Long Y, Corces MR, Granja JM, Mundlos S, Cech TR, Boettiger A, Others, Polycomb-mediated genome architecture enables long-range spreading of H3K27 methylation. BioRXiv (2020).
15. Dormidontova EE, Grosberg AY, Khokhlov AR, Intramolecular phase separation of a copolymer chain with mobile primary structure. Macromolecular Theory Simulations. 1, 375–385 (1992).
16. Michieletto D, Orlandini E, Marenduzzo D, Polymer model with epigenetic recoloring reveals a pathway for the de novo establishment and 3D organization of chromatin domains. Physical Review X. 6, 041047 (2016).
17. Cortini R, Barbi M, Caré BR, Lavelle C, Lesne A, Mozziconacci J, Victor J-M, The physics of epigenetics. Rev. Mod. Phys 88, 025002 (2016).
18. Jost D, Vaillant C, Epigenomics in 3D: importance of long-range spreading and specific interactions in epigenomic maintenance. Nucleic Acids Res. 46, 2252–2264 (2018). [PubMed: 29365171]
19. Erdel F, Greene EC, Generalized nucleation and looping model for epigenetic memory of histone modifications. Proceedings of the National Academy of Sciences. 113, E4180–E4189 (2016).

20. Sandholtz SH, MacPherson Q, Spakowitz AJ, Physical modeling of the heritability and maintenance of epigenetic modifications. Proceedings of the National Academy of Sciences. 117, 20423–20429 (2020).
21. Katava M, Shi G, Thirumalai D, Chromatin dynamics controls epigenetic domain formation. bioRxiv (2021).
22. Michieletto D, Chiang M, Coli D, Papantonis A, Orlandini E, Cook PR, Marenduzzo D, Shaping epigenetic memory via genomic bookmarking. Nucleic Acids Res. 46, 83–93 (2018). [PubMed: 29190361]
23. Abdulla AZ, Vaillant C, Jost D, Painters in chromatin: a unified quantitative framework to systematically characterize epigenome regulation and memory. Nucleic Acids Res. 50, 9083–9104 (2022). [PubMed: 36018799]
24. Bauer H, Structure and arrangement of salivary gland chromosomes in Drosophila species. Proceedings of the National Academy of Sciences. 22, 216–222 (1936).
25. Strom AR, Emelyanov AV, Mir M, Fyodorov DV, Darzacq X, Karpen GH, Phase separation drives heterochromatin domain formation. Nature. 547, 241–245 (2017). [PubMed: 28636597]
26. Larson AG, Elnatan D, Keenen MM, Trnka MJ, Johnston JB, Burlingame AL, Agard DA, Redding S, Narlikar GJ, Liquid droplet formation by HP1α suggests a role for phase separation in heterochromatin. Nature. 547, 236–240 (2017). [PubMed: 28636604]
27. Falk M, Feodorova Y, Naumova N, Imakaev M, Lajoie BR, Leonhardt H, Joffe B, Dekker J, Fudenberg G, Solovei I, Others, Heterochromatin drives compartmentalization of inverted and conventional nuclei. Nature. 570, 395–399 (2019). [PubMed: 31168090]
28. Strickfaden H, Zunhammer A, van Koningsbruggen S, Köhler D, Cremer T, 4D chromatin dynamics in cycling cells: Theodor Boveri's hypotheses revisited. Nucleus. 1, 284–297 (2010). [PubMed: 21327076]
29. Kadoch C, Williams RT, Calarco JP, Miller EL, Weber CM, Braun SMG, Pulice JL, Chory EJ, Crabtree GR, Dynamics of BAF-Polycomb complex opposition on heterochromatin in normal and oncogenic states. Nat. Genet 49, 213–222 (2017). [PubMed: 27941796]
30. Dobrinić P, Szczurek AT, Klose RJ, PRC1 drives Polycomb-mediated gene repression by controlling transcription initiation and burst frequency. Nat. Struct. Mol. Biol 28, 811–824 (2021). [PubMed: 34608337]
31. Gabriele M, Brandão HB, Grosse-Holz S, Jha A, Dailey GM, Cattoglio C, Hsieh T-HS, Mirny L, Zechner C, Hansen AS, Dynamics of CTCF-and cohesin-mediated chromatin looping revealed by live-cell imaging. Science. 376, 496–501 (2022). [PubMed: 35420890]
32. Ito K, Zaret KS, Maintaining transcriptional specificity through mitosis. Annu. Rev. Genomics Hum. Genet 23, 53–71 (2022). [PubMed: 35440147]
33. Liu Y, Pelham-Webb B, Di Giammartino DC, Li J, Kim D, Kita K, Saiz N, Garg V, Doane A, Giannakakou P, Hadjantonakis A-K, Elemento O, Apostolou E, Widespread mitotic bookmarking by histone marks and transcription factors in pluripotent stem cells. Cell Rep. 19, 1283–1293 (2017). [PubMed: 28514649]
34. Rea S, Eisenhaber F, O'Carroll D, Strahl BD, Sun ZW, Schmid M, Opravil S, Mechtler K, Ponting CP, Allis CD, Jenuwein T, Regulation of chromatin structure by site-specific histone H3 methyltransferases. Nature. 406, 593–599 (2000). [PubMed: 10949293]
35. Lau PNI, Cheung P, Histone code pathway involving H3 S28 phosphorylation and K27 acetylation activates transcription and antagonizes polycomb silencing. Proc. Natl. Acad. Sci. U. S. A 108, 2801–2806 (2011). [PubMed: 21282660]
36. Pastor-Satorras R, Castellano C, Van Mieghem P, Vespignani A, Epidemic processes in complex networks. Rev. Mod. Phys 87, 925 (2015).
37. Stafford JM, Lee C-H, Voigt P, Descostes N, Saldaña-Meyer R, Yu J-R, Leroy G, Oksuz O, Chapman JR, Suarez F, Others, Multiple modes of PRC2 inhibition elicit global chromatin alterations in H3K27M pediatric glioma. Science advances. 4, eaau5935 (2018).
38. Leicher R, Eva JG, Lin X, Reynolds MJ, Xie W, Walz T, Zhang B, Muir TW, Liu S, Single-molecule and in silico dissection of the interaction between Polycomb repressive complex 2 and chromatin. Proceedings of the National Academy of Sciences. 117, 30465–30475 (2020).

39. Gillespie MA, Palii CG, Sanchez-Taltavull D, Shannon P, Longabaugh WJR, Downes DJ, Sivaraman K, Espinoza HM, Hughes JR, Price ND, Perkins TJ, Ranish JA, Brand M, Absolute Quantification of Transcription Factors Reveals Principles of Gene Regulation in Erythropoiesis. Mol. Cell 78, 960–974.e11 (2020). [PubMed: 32330456]
40. Johnson KA, Goody RS, The original Michaelis constant: translation of the 1913 Michaelis--Menten paper. Biochemistry. 50, 8264–8269 (2011). [PubMed: 21888353]
41. Gunawardena J, Time-scale separation--Michaelis and Menten's old idea, still bearing fruit. FEBS J. 281, 473–488 (2014). [PubMed: 24103070]
42. Bancaud A, Huet S, Daigle N, Mozziconacci J, Beaudouin J, Ellenberg J, Molecular crowding affects diffusion and binding of nuclear proteins in heterochromatin and reveals the fractal organization of chromatin. EMBO J. 28, 3785–3798 (2009). [PubMed: 19927119]
43. McCabe MT, Ott HM, Ganji G, Korenchuk S, Thompson C, Van Aller GS, Liu Y, Graves AP, Della Pietra A 3rd, Diaz E, LaFrance LV, Mellinger M, Duquenne C, Tian X, Kruger RG, McHugh CF, Brandt M, Miller WH, Dhanak D, Verma SK, Tummino PJ, Creasy CL, EZH2 inhibition as a therapeutic strategy for lymphoma with EZH2-activating mutations. Nature. 492, 108–112 (2012). [PubMed: 23051747]
44. Béguelin W, Teater M, Meydan C, Hoehn KB, Phillip JM, Soshnev AA, Venturutti L, Rivas MA, Calvo-Fernández MT, Gutierrez J, Camarillo JM, Takata K, Tarte, Kelleher NL, Steidl C, Mason CE, Elemento O, Allis CD, Kleinstein SH, Melnick AM, Mutant EZH2 induces a pre-malignant lymphoma niche by reprogramming the immune response. Cancer Cell. 37, 655–673.e11 (2020). [PubMed: 32396861]
45. Souroullas GP, Jeck WR, Parker JS, Simon JM, Liu J-Y, Paulk J, Xiong J, Clark KS, Fedoriw Y, Qi J, Burd CE, Bradner JE, Sharpless NE, An oncogenic Ezh2 mutation induces tumors through global redistribution of histone 3 lysine 27 trimethylation. Nat. Med 22, 632–640 (2016). [PubMed: 27135738]
46. Diehl KL, Ge EJ, Weinberg DN, Jani KS, Allis CD, Muir TW, PRC2 engages a bivalent H3K27M-H3K27me3 dinucleosome inhibitor. Proc. Natl. Acad. Sci. U. S. A 116, 22152–22157 (2019). [PubMed: 31611394]
47. Ou HD, Phan S, Deerinck TJ, Thor A, Ellisman MH, O'shea CC, ChromEMT: Visualizing 3D chromatin structure and compaction in interphase and mitotic cells. Science. 357, eaag0025 (2017).
48. Murphy S, Boettiger AN, Polycomb repression of Hox genes involves spatial feedback but not domain compaction or demixing. bioRxiv (2022), p. 2022.10.14.512199, doi:10.1101/2022.10.14.512199.
49. Alabert C, Barth TK, Reverón-Gómez N, Sidoli S, Schmidt A, Jensen ON, Imhof A, Groth A, Two distinct modes for propagation of histone PTMs across the cell cycle. Genes Dev. 29, 585–590 (2015). [PubMed: 25792596]
50. Elgin SCR, Reuter G, Position-effect variegation, heterochromatin formation, and gene silencing in Drosophila. Cold Spring Harb. Perspect. Biol 5, a017780 (2013). [PubMed: 23906716]
51. Weber CM, Hafner A, Kirkland JG, Braun SMG, Stanton BZ, Boettiger AN, Crabtree GR, mSWI/SNF promotes Polycomb repression both directly and through genome-wide redistribution. Nat. Struct. Mol. Biol 28, 501–511 (2021). [PubMed: 34117481]
52. Conway E, Rossi F, Fernandez-Perez D, Ponzo E, Ferrari KJ, Zanotti M, Manganaro D, Rodighiero S, Tamburri S, Pasini D, BAP1 enhances Polycomb repression by counteracting widespread H2AK119ub1 deposition and chromatin condensation. Mol. Cell 81, 3526–3541.e8 (2021). [PubMed: 34186021]
53. Zhang X, Liu X, Du Z, Wei L, Fang H, Dong Q, Niu J, Li Y, Gao J, Zhang MQ, Xie W, Wang X, The loss of heterochromatin is associated with multiscale three-dimensional genome reorganization and aberrant transcription during cellular senescence. Genome Res. 31, 1121–1135 (2021). [PubMed: 34140314]
54. Olan I, Narita M, Senescence: An Identity Crisis Originating from Deep Within the Nucleus. Annu. Rev. Cell Dev. Biol 38, 219–239 (2022). [PubMed: 35804478]

55. Thakore PI, D'ippolito AM, Song L, Safi A, Shivakumar NK, Kabadi AM, Reddy TE, Crawford GE, Gersbach CA, Highly specific epigenome editing by CRISPR-Cas9 repressors for silencing of distal regulatory elements. Nat. Methods 12, 1143–1149 (2015). [PubMed: 26501517]
56. Pulecio J, Verma N, Mejía-Ramírez E, Huangfu D, Raya A, CRISPR/Cas9-based engineering of the epigenome. Cell Stem Cell. 21, 431–447 (2017). [PubMed: 28985525]
57. Yang H, Berry S, Olsson TSG, Hartley M, Howard M, Dean C, Distinct phases of Polycomb silencing to hold epigenetic memory of cold in Arabidopsis. Science. 357, 1142–1145 (2017). [PubMed: 28818969]
58. Lövkvist C, Mikulski P, Reeck S, Hartley M, Dean C, Howard M, Hybrid protein assembly-histone modification mechanism for PRC2-based epigenetic switching and memory. Elife. 10 (2021).
59. Preissl S, Gaulton KJ, Ren B, Characterizing cis-regulatory elements using single-cell epigenomics. Nat. Rev. Genet, 1–23 (2022). [PubMed: 34782779]
60. Lu BY, Bishop CP, Eissenberg JC, Developmental timing and tissue specificity of heterochromatin-mediated silencing. EMBO J. 15, 1323–1332 (1996). [PubMed: 8635465]
61. Bughio F, Huckell GR, Maggert KA, Monitoring of switches in heterochromatin-induced silencing shows incomplete establishment and developmental instabilities. Proc. Natl. Acad. Sci. U. S. A 116, 20043–20053 (2019). [PubMed: 31527269]
62. Schmitges FW, Prusty AB, Faty M, Stützer A, Lingaraju GM, Aiwazian J, Sack R, Hess D, Li L, Zhou S, Bunker RD, Wirth U, Bouwmeester T, Bauer A, Ly-Hartig N, Zhao, Chan H, Gu J, Gut H, Fischle W, Müller J, Thomä NH, Histone methylation by PRC2 is inhibited by active chromatin marks. Mol. Cell 42, 330–341 (2011). [PubMed: 21549310]
63. Henikoff S, Shilatifard A, Histone modification: cause or cog? Trends Genet. 27, 389–396 (2011). [PubMed: 21764166]
64. Berry S, Dean C, Howard M, Slow chromatin dynamics allow polycomb target genes to filter fluctuations in transcription factor activity. Cell systems. 4, 445–457 (2017). [PubMed: 28342717]
65. Lövkvist C, Howard M, Using computational modelling to reveal mechanisms of epigenetic Polycomb control. Biochem. Soc. Trans 49, 71–77 (2021). [PubMed: 33616630]
66. Coleman RT, Struhl G, Causal role for inheritance of H3K27me3 in maintaining the OFF state of a Drosophila HOX gene. Science. 356 (2017), doi:10.1126/science.aai8236.
67. Shafiq TA, Moazed D, Three rules for epigenetic inheritance of human Polycomb silencing. bioRxiv (2023), p. 2023.02.27.530239, doi:10.1101/2023.02.27.530239.
68. Shumaker DK, Dechat T, Kohlmaier A, Adam SA, Bozovsky MR, Erdos MR, Eriksson M, Goldman AE, Khuon S, Collins FS, Jenuwein T, Goldman RD, Mutant nuclear lamin A leads to progressive alterations of epigenetic control in premature aging. Proc. Natl. Acad. Sci. U. S. A 103, 8703–8708 (2006). [PubMed: 16738054]
69. Karoutas A, Akhtar A, Functional mechanisms and abnormalities of the nuclear lamina. Nat. Cell Biol 23, 116–126 (2021). [PubMed: 33558730]
70. Pande VS, Grosberg AY, Tanaka T, Heteropolymer freezing and design: Towards physical models of protein folding. Rev. Mod. Phys 72, 259–314 (2000).
71. Grosberg AY, Khokhlov AR, Giant molecules: Here, there, and everywhere (2nd edition) (World Scientific Publishing, Singapore, Singapore, 2010).
72. Fink TM, Ball RC, How many conformations can a protein remember? Phys. Rev. Lett 87, 198103 (2001). [PubMed: 11690459]
73. Shakhnovich EI, Gutin AM, Engineering of stable and fast-folding sequences of model proteins. Proc. Natl. Acad. Sci. U. S. A 90, 7195–7199 (1993). [PubMed: 8346235]
74. Pande VS, Grosberg AY, Tanaka T, Thermodynamic procedure to synthesize heteropolymers that can renature to recognize a given target molecule. Proc. Natl. Acad. Sci. U. S. A 91, 12976–12979 (1994). [PubMed: 7809158]
75. Hopfield JJ, Neural networks and physical systems with emergent collective computational abilities. Proceedings of the national academy of sciences. 79, 2554–2558 (1982).
76. Hebb DO, The Organization of Behavior, McGill University (1949).
77. Löwel S, Singer W, Selection of intrinsic horizontal connections in the visual cortex by correlated neuronal activity. Science. 255, 209–212 (1992). [PubMed: 1372754]

78. Dexter JP, Prabakaran S, Gunawardena J, A complex hierarchy of avoidance behaviors in a single-cell eukaryote. Curr. Biol 29, 4323–4329 (2019). [PubMed: 31813604]

79. Gershman SJ, Balbi PEM, Gallistel CR, Gunawardena J, Reconsidering the evidence for learning in single cells. Elife. 10, e61907 (2021). [PubMed: 33395388]

80. Kramar M, Alim K, Encoding memory in tube diameter hierarchy of living flow network. Proc. Natl. Acad. Sci. U. S. A 118 (2021), doi:10.1073/pnas.2007815118.

81. Murugan A, Zeravcic Z, Brenner MP, Leibler S, Multifarious assembly mixtures: Systems allowing retrieval of diverse stored structures. Proceedings of the National Academy of Sciences. 112, 54–59 (2015).

82. Zhong W, Schwab DJ, Murugan A, Associative pattern recognition through macromolecular self-assembly. J. Stat. Phys 167, 806–826 (2017).

83. Imakaev M, Goloborodko A, Brandão HB, mirnylab/polychrom: v0.1.0 (2019), doi:10.5281/ZENODO.3579473.

84. Eastman P, Swails J, Chodera JD, McGibbon RT, Zhao Y, Beauchamp KA, Wang L-P, Simmonett AC, Harrigan MP, Stern CD, Others, OpenMM 7: Rapid development of high performance algorithms for molecular dynamics. PLoS Comput. Biol 13, e1005659 (2017). [PubMed: 28746339]

85. Miller JC, Ting T, EoN (Epidemics on Networks): a fast, flexible Python package for simulation, analytic approximation, and analysis of epidemics on networks. Journal of Open Source Software. 4, 1731 (2019).

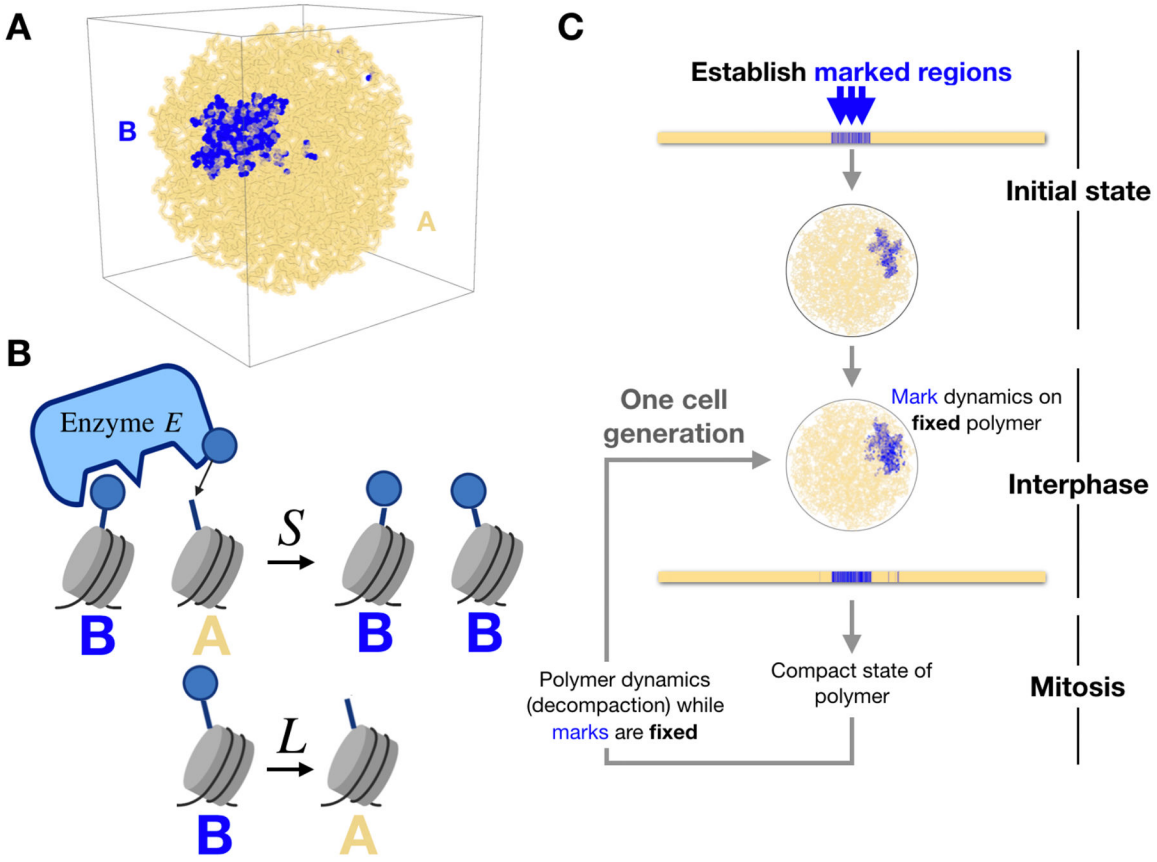


**Fig. 1. Model of mark and chromatin dynamics.**

**(A)** Chromatin in the nucleus modeled as a spherically confined copolymer with monomers of two types, A (pale yellow) and B (blue), representing a varying pattern of histone marks. Monomers of type B, which represent regions bearing heterochromatic marks, self-attract. **(B)** Marks spread to 3D neighbors at rate *S*, and are lost everywhere uniformly at rate *L*. **(C)** The overall dynamics of our model consist of alternating phases of polymer dynamics and mark dynamics, representing the cell cycle.

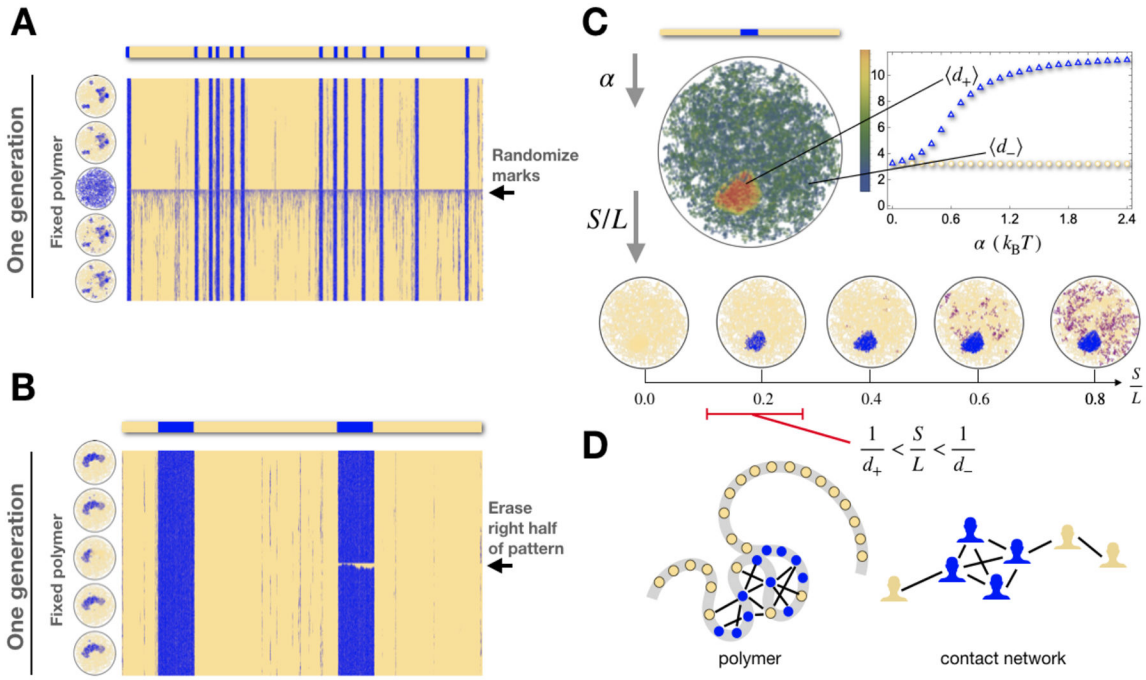


**Fig. 2. Spreading marks sharply localize to dense regions.**

**(A)** Mark dynamics (with $S/L = 0.5$) over a single cell generation, on a fixed polymer folded according to an initial pattern (with $\alpha = 2.4\ k_B T$). Time advances from top to bottom. Inset circles (left) show snapshots of the polymer configuration (2D projection) over time. **(B)** As in (A), with a different initial pattern and perturbation. **(C)** Top: when the polymer folds, marked regions tend to be denser (red) than unmarked ones (green), due to the self-attraction of marks. The plot shows the average number of monomer neighbors in each compartment as a function of the strength of B-B self-attraction α. Bottom: in turn, when marks evolve according to their dynamics of spreading and loss, they tend to localize in dense regions for a range of $S/L$ values. **(D)** An analogy to epidemic spreading, where marked monomers are equivalent to infected people, predicts correctly that this localization will occur *at least* in the red interval, whose width is set by the number of neighbors in each region.

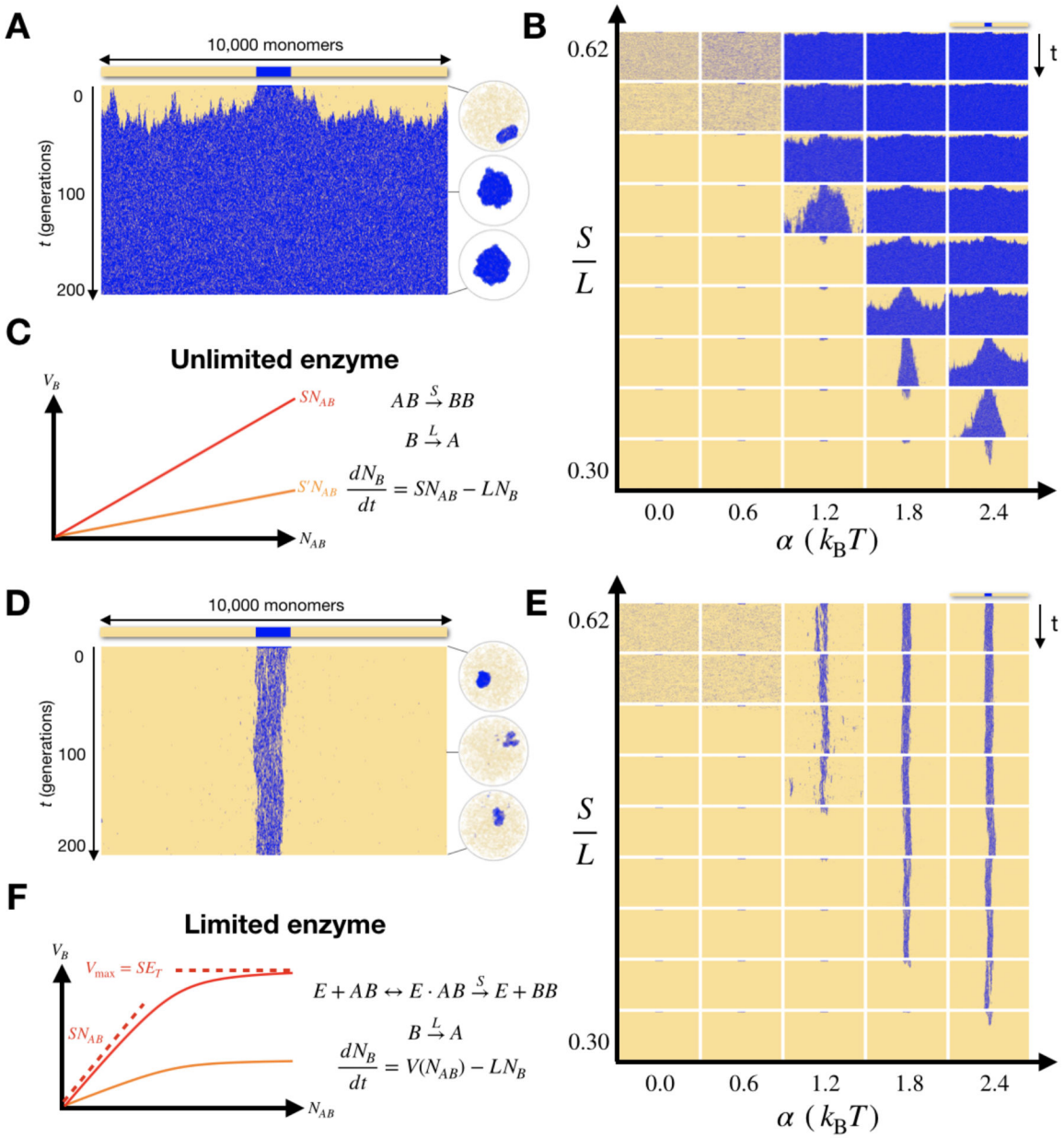


**Fig. 3. Limited enzyme stabilizes memory over multiple generations.**

**(A)** Time evolution of a mark pattern, with unlimited enzyme, over 200 generations ($\alpha$ = *2.4* $k_B T$, *S/L* = 0.42), starting from an initial pattern consisting of a single domain of 1000 marked monomers. Inset circles show snapshots in time of the polymer configuration. For this choice of parameter marks spread everywhere and the polymer collapses. **(B)** Time evolution of the mark pattern, with unlimited enzyme, as a function of $\alpha$ and *S/L*. No stable memory. **(C)** With unlimited enzyme, the global marking rate in the nucleus $V_B$ is proportional to the number $N_{AB}$ of A-B pairs. **(D)** and **(E)**, just as in (A) and (B), but with limited enzyme, $E_T$ = 1000. Stable memory is achieved for hundreds of generations, over a broad range of parameters. **(F)** With limited enzyme, $V_B$ is proportional to $N_{AB}$ when it

is small, but then saturates at the value $V_{max} = SE_T$, preventing uncontrolled spreading of marks.

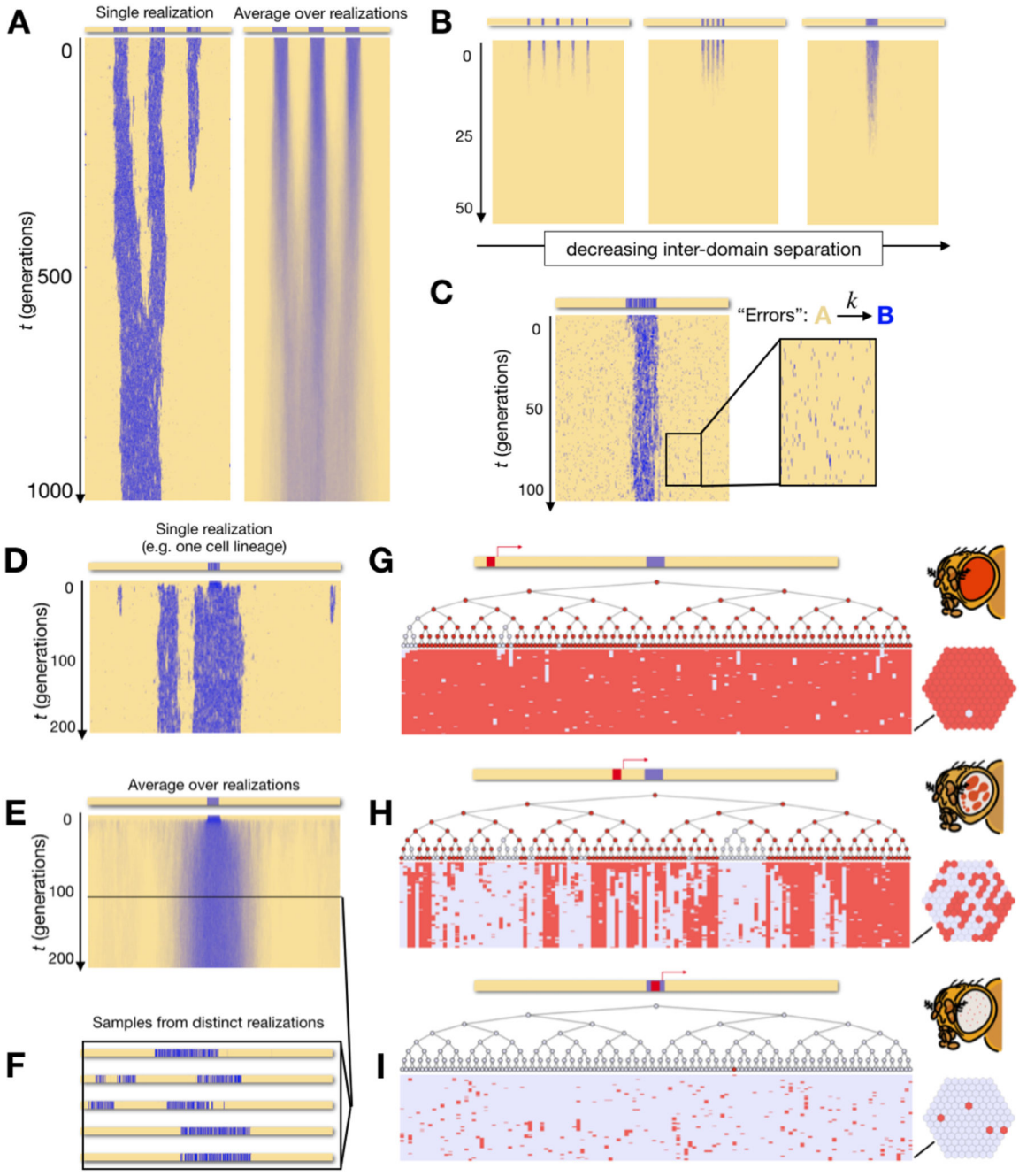


**Fig. 4. Dynamics of complex patterns and position-effect variegation.**

**(A)** Time evolution of a pattern consisting of three, equally-sized mark domains ($\alpha$ = 2.4 $k_B T$, $S/L$ = 0.5, $E_T$ = 3000). The pattern is stable for hundreds of generations, though marks eventually redistribute to form a single contiguous domain. In a population average (right) the three domains instead appear to merge. **(B)** Multiple small domains (population average shown) competing with a much bigger one (not pictured) survive redistribution longer the closer they are together. **(C)** Error correction: tiny "domains" introduced by spontaneous marking at a rate $k$ are lost immediately ($\alpha$ = 2.4 $k_B T$, $S/L$ = 0.5, $E_T$ = 1000, $k/L$ = 0.003). **(D)** Expansion of marks from a small domain leads to the random formation of new domains

that can be remembered for hundreds of generations ($a$ = 2.4 $k_B T$, $S/L$ = 0.5, $E_T$ = 3000). **(E)** The population average of (D) hides the large cell variation **(F)**. **(G-I)** Position-effect variegation: To visualize the consequences of this, we consider a gene "regulatory region" of five consecutive monomers (red), somewhere along the polymer, and take the presence of a single B monomer in this region to silence the gene. Investigating silencing status (white = silenced, red = not silenced) in a lineage tree generated with our model, we find different phenotypes reminiscent of the classic position-effect variegation: (G) wild-type, (H) "sectored" variegation, and (I) "salt-and-pepper" variegation, depending on the position of the regulatory region.